ON THE RECEPTIVITY OF SUPERSONIC BOUNDARY LAYER TO OSCILLATING MACH WAVES

Shoji Sakaue*, Michio Nishioka*
***Dept. Aerospace Eng., Osaka Prefecture University**

Keywords: *Supersonic Boundary Layer Instability, Receptivity, Oscillating Mach wave*

Abstract

The present paper describes our numerical study of supersonic boundary layer receptivity to Mach waves incident onto leading edge at freestream Mach number 2.2. We examine the external disturbance field around the leading edge in detail to clarify the formation of oscillating Stokes layer and its evolution into T-S wave. The results show that the amplitude ratio of the excited T-S wave to the Stokes layer in the vicinity of the leading edge is almost of unity.

1 Introduction

The present study is concerned with the receptivity process in supersonic boundary layer flow. Here, the receptivity means the flow process by which external disturbances generate eigenmode waves (such as T-S waves). For incompressible flow, as stated by Nishioka and Morkovin[1], since external disturbances in the freestream (acoustic noise) have generally much longer wavelength than that of the T-S wave with the corresponding frequency, the wavelength conversion is crucial for the generation of T-S waves. Such conversion can occur, for instance, at a local place where the flow undergoes rapid streamwise variations (leading edge region and/or regions with abrupt changes in wall geometry). When external disturbances impose unsteady pressure gradients on the wall, they simultaneously generate fluctuating vorticities of the same temporal and spatial scales. Nishioka and Morkovin[1] clarified that external disturbances should cause x-dependent Stokes layer which contains the wave number components corresponding to the T-S wave to be generated. For compressible flow, we examined the excitation of the T-S wave for supersonic boundary layer at a freestream Mach number 2.2 through direct numerical simulations[2] and clarified that the intensity of the excited T-S wave is proportional to that of the T-S wavenumber spectrum contained in the x-dependent Stokes layer induced by a oscillating streamwise velocity component on the narrow strip of the wall just like as in the corresponding incompressible flow case[3].

In supersonic cases, the gap in the phase speeds is much reduced between freestream disturbances (Mach waves) and boundary layer instabilities as both are of the same order as the freestream velocity. However the phase speeds of the instability waves, at least in the region of growth, always lie between the sonic speed and the freestream, the wavelengths of the external disturbances never exactly match those of the boundary layer instabilities. Thus, a conversion mechanism is still necessary to accomplish energy transfer from the freestream Mach waves to the instability waves[4] and the receptivity in the leading edge region is quite important in supersonic boundary layers, too. Hence, for the case of supersonic flow, many studies have been made through theoretical[5,6], experimental[7, 8] and numerical[9~13] approaches for the boundary layer receptivity to incident Mach waves. However, the supersonic receptivity has not been clarified yet. This is mainly because, for the case of the oscillating Mach wave

incident onto boundary layer, the forced waves appear and persist long to make the excited flow complex, and it is rather hard to singled out the T-S waves from the total fluctuations contaminated by the forced waves.

This paper describes our numerical simulations made to clarify the supersonic boundary layer receptivity to time periodic Mach waves incident onto the leading edge.

2 Numerical Scheme

We consider supersonic two-dimensional boundary layer on a flat plate at freestream Mach number $M_\infty = 2.2$. The origin of the coordinates is set at the leading edge of the boundary layer plate, the x-axis is in the streamwise direction and the y-axis is perpendicular to the wall. The governing equations are the two-dimensional compressible Navier-Stokes equations non-dimensionalized by using the freestream velocity U_∞, density ρ_∞, viscosity μ_∞ and the displacement thickness δ_1 at $x = 40$.

$$\frac{\partial Q}{\partial t} + \frac{\partial F_i}{\partial x_i} = \frac{\partial F_{vi}}{\partial x_i} \tag{1}$$

$$Q = \begin{pmatrix} \rho \\ \rho u_1 \\ \rho u_2 \\ e \end{pmatrix}, \quad F_i = \begin{pmatrix} \rho u_i \\ \rho u_1 u_i + p\delta_{1i} \\ \rho u_2 u_i + p\delta_{2i} \\ (e+p)\,u_i \end{pmatrix},$$

$$F_{vi} = \frac{1}{Re}\begin{pmatrix} 0 \\ \tau_{1i} \\ \tau_{2i} \\ q_i + u_j \tau_{ij} \end{pmatrix}$$

The viscous stress tensor τ_{ij} and the heat flux vector q_i are respectively written as follows:

$$\tau_{ij} = \mu\left(\frac{\partial u_i}{\partial x_j} + \frac{\partial u_j}{\partial x_i} - \frac{2}{3}\delta_{ij}\frac{\partial u_k}{\partial x_k}\right) \tag{2}$$
$$q_i = \frac{\mu}{Pr}\cdot\frac{\gamma}{\gamma-1}\cdot\frac{\partial T}{\partial x_i}$$

Here, γ denotes the ratio of specific heat. The Reynolds number defined by $Re = \rho_\infty U_\infty \delta_1/\mu_\infty$ is taken as 650. The viscosity coefficient μ is assumed to be proportional to the temperature T. The Prandtl number Pr is assumed to be constant (= 1.0).

The computational domain of the present simulations is $-5 \le x \le 140$, $-24 \le y \le 24$. The domain is divided into upper and lower parts, and each part is divided into two sections for saving the memory and the computational time. The first section extends from $x = -5$ to $x = 40$, the second section from $x = 30$ to $x = 140$. The grid sizes for these two sections are 1620×520 and 1120×520, respectively. The smallest grid size around the leading edge is taken to be $\Delta x = \Delta y = 0.005$, thus the Reynolds number based on the smallest grid is 3.25.

The governing equations are solved numerically by the third-order upwind TVD scheme[14] for the convection terms and the second-order central difference scheme for the other spatial derivatives. For the time advancement, the second-order explicit Euler scheme is used. Boundary conditions for the computation are given by prescribed variables on the upstream boundary, no-slip adiabatic walls on solid surfaces, and the zeroth order extrapolation on the upper/lower and downstream boundaries.

The oscillating Mach wave is radiated from a local suction/blowing slot perpendicular to the flow direction, being periodic with angular frequency ω, and the intensity of the disturbance source $v(x)$ is given by the following equation,

$$v(x) = \begin{cases} A_w \cos^2\left(\dfrac{\pi(x-x_0)}{2s}\right) & : |x-x_0| \le s \\ 0 & : |x-x_0| > s \end{cases} \tag{4}$$

thus it has the length scale $2s$. In the present paper, $2s$ is selected to be 4.0 and 18.0. And the center of the disturbance source (x_0, y_0) is set at the position where the Mach line from the center runs through the leading-edge of the boundary layer plate. The intensity of disturbance source A_w is fixed at 0.2% of U_∞.

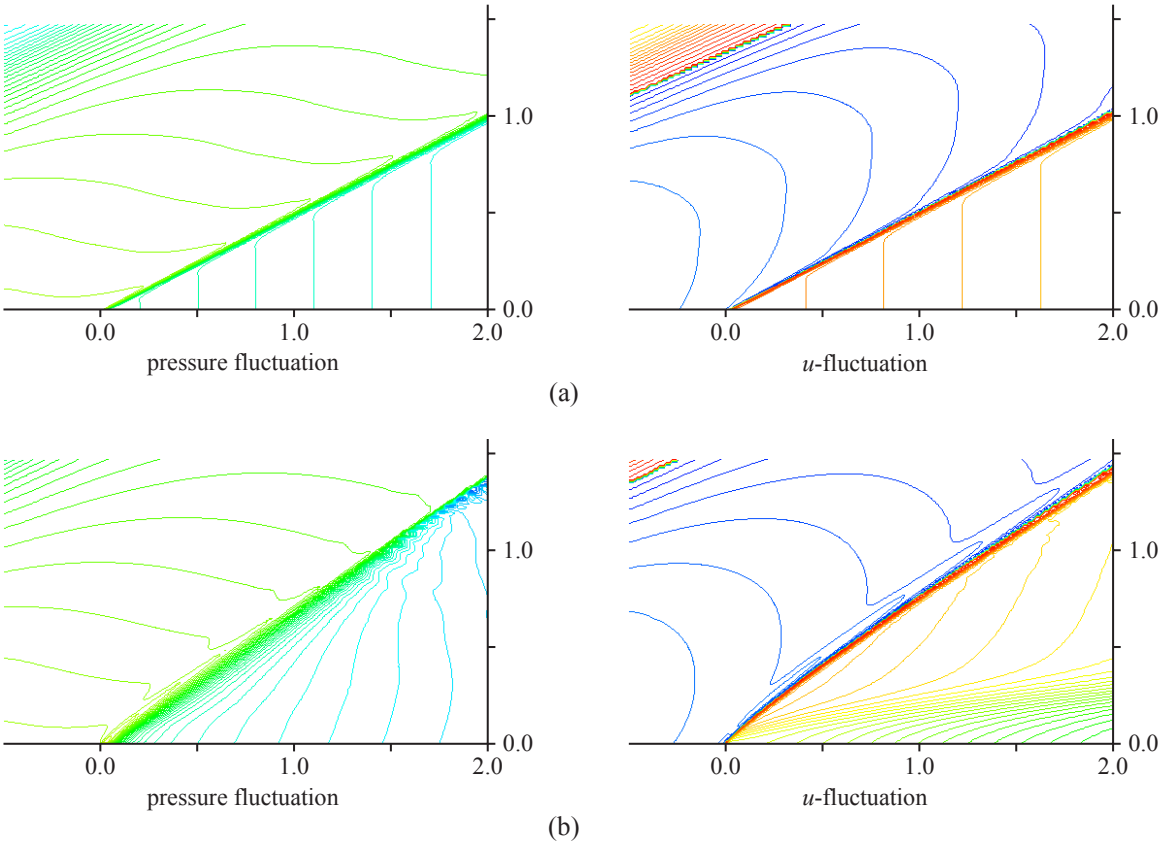

Fig.1 Pressure and u-fluctuations around the leading edge illustrated by contour map of the phase of fluctuations; (a) inviscid flow, (b) viscous flow.

The angular frequency ω is taken to be 0.18. For the T-S wave with $\omega = 0.18$, whose growth rate is maximum at $x = 60$, the eigenvalue α is calculated to be $0.2766 - \mathbf{i}\ 0.1344 \times 10^{-2}$ at $x = 60$, the corresponding wave length λ being 22.71.

3 Results

In the present paper, we will describe our simulation results for the following four cases.

	$2s$	(x_0, y_0)
Case1	4.0	(−23.5, −12.0)
Case2	4.0	(−105.8, −54.0)
Case3	18.0	(−23.5, −12.0)
Case4	18.0	(−105.8, −54.0)

However, we pay attention only to the excited fluctuations on the upper side of the plate, and mainly describe the result for case2.

First of all, we will describe the fluctuation field near the leading edge. Fig.1 show the pressure p and streamwise velocity u fluctuations around the leading edge illustrated by contour map of the phase of the fluctuations. Fig.1 (a) shows the simulation result for the inviscid flow. As seen from the figure, the fluctuation field is divided into two parts by the Mach line running through the leading edge. The fluctuation propagates along the Mach line in the region upstream and above it, while the fluctuation on the wall propagates as plane wave parallel to the plate because of the uniform mean flow and the boundary condition on the wall. Fig.1 (b) shows the simulation result for

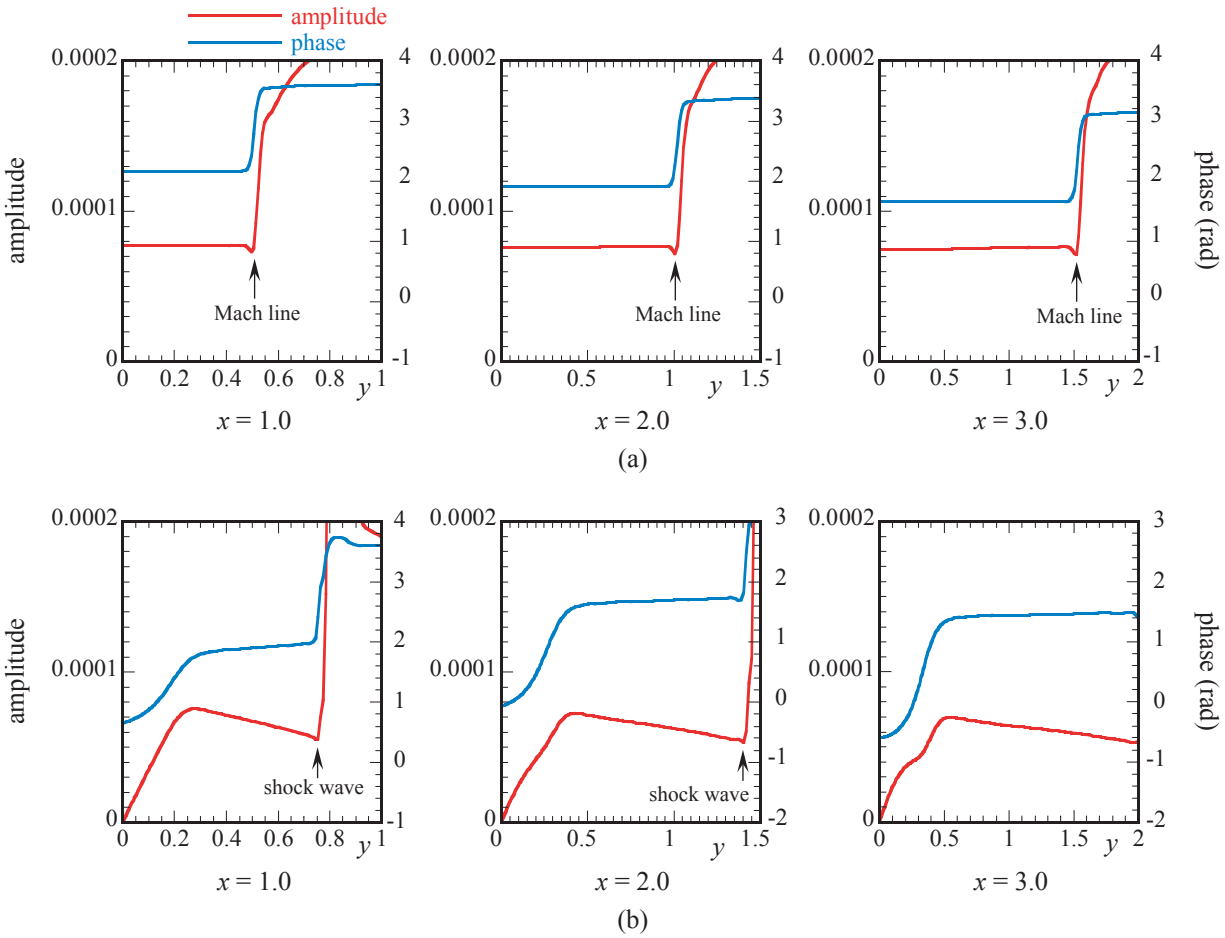

Fig.2 y-distributions of amplitude and phase of u-fluctuations near the leading edge: (a) inviscid flow, (b) viscous flow.

the viscous flow. As we see from the comparison with Fig.1 (a), the phase distribution of pressure fluctuation slightly changes from the result of the inviscid flow due to the leading edge shock wave and the boundary layer development along the plate, but it also propagates almost as the plane wave.

Fig.2 show the y-distributions of amplitude and phase of u-fluctuation near the leading edge. Fig.2 (a) shows the result for the inviscid flow and Fig.2 (b), the result for the viscous flow. We see from Fig.2 (b) that the amplitude distribution has a local maximum near the outer edge of the boundary layer and the phase lag decreases toward the wall. The oscillating Stokes layer is induced by the incident Mach waves just behind the leading edge. The amplitude of u-fluctuation of the Stokes layer corresponds to the amplitude of u-fluctuation on the wall for the inviscid flow as shown in Fig.2 (a).

To examine the excited fluctuations, the streamwise variations of amplitude and phase of the u-fluctuation on the wall for the case of the inviscid flow and the vorticity fluctuation on the wall for the case of the viscous flow are illustrated in Fig.3. In these figures, red lines indicate the T-S wave behavior predicted from the linear stability analysis. The result for the inviscid flow shows that the fluctuation consists

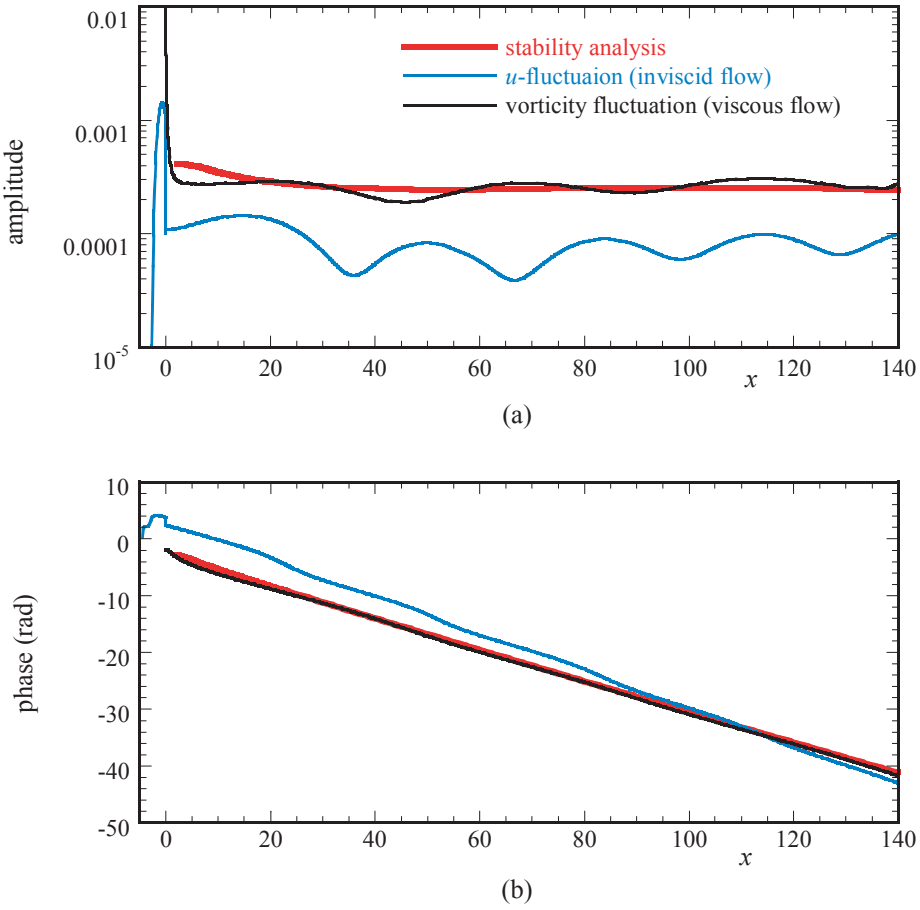

Fig.3 Streamwise variations of (a) amplitude and (b) phase of u-fluctuation on the wall for the inviscid flow and the vorticity fluctuation on the wall for the viscous flow. Red lines represent the result from linear stability analysis.

of two waves with the phase velocity $1-1/M_\infty$ and $1+1/M_\infty$. As seen from the figure, though the streamwise variation of amplitude of the vorticity fluctuation on the wall slightly undulates due to the existence of the external disturbance, both amplitude and phase variations on the wall agree well with the result from the linear stability analysis and clearly show that the excited fluctuation in the boundary layer is governed by T-S wave.

To examine the generation of T-S wave, Fig.4 show the y-distributions of amplitude and phase of u-fluctuation up to $x = 120$ for the case of the viscous flow. In these figures, red lines indicate the T-S wave profile calculated from the linear stability analysis. The oscillating Stokes layer is rapidly developing into T-S wave type even at $x = 5.0$ and establishes itself as the T-S wave at $x \geq 10.0$, which is corresponding to a half wavelength from the leading edge.

Here, it is important to note that the excited fluctuations in the upper side boundary layer show almost the same behavior for all the cases we examined in the present study.

To see what actually determines the amplitude of excited T-S wave, Table 1 summarizes the u-fluctuation amplitudes of oscillating Mach wave (A_M), the maximum u-fluctuation amplitudes of the Stokes layers

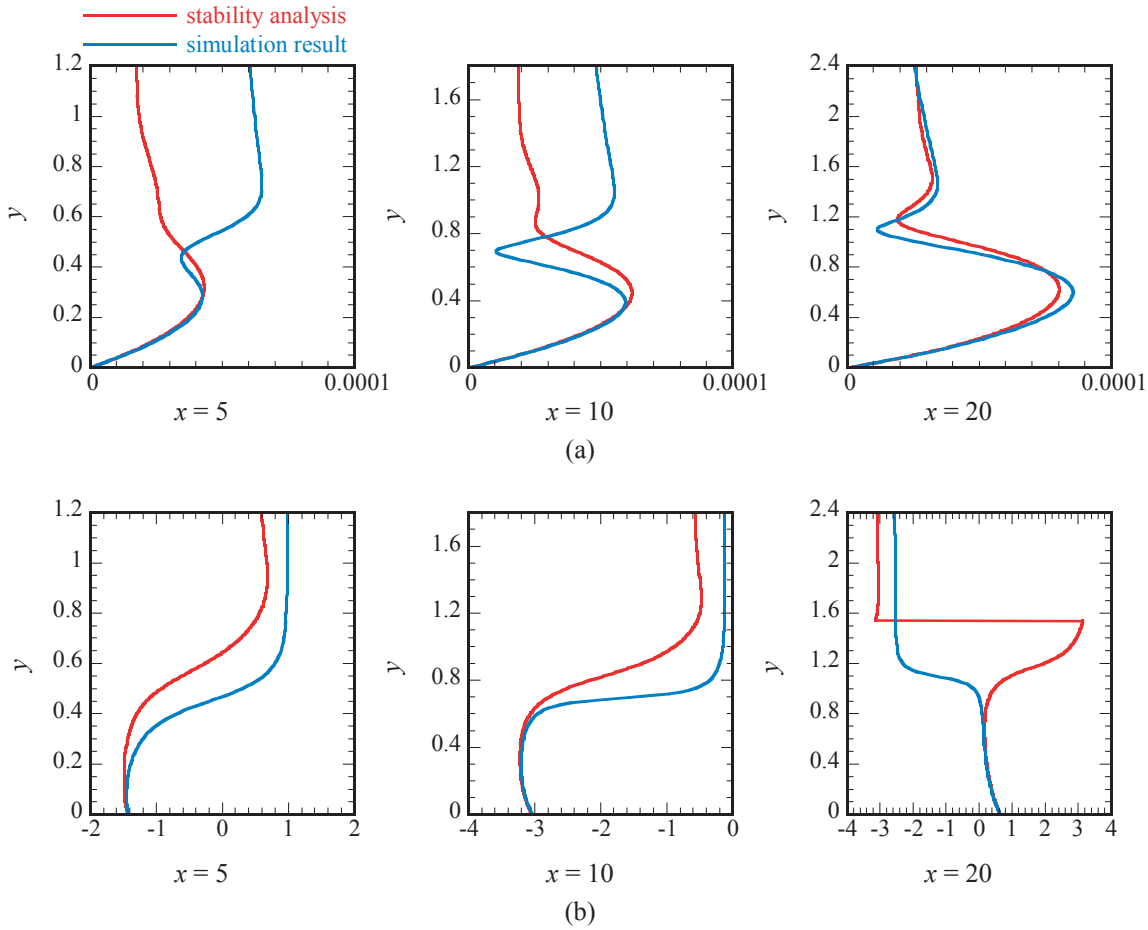

Fig.4 y-distributions of (a) amplitude and (b) phase of u-fluctuations for the viscous flow. Red lines represent the result from linear stability analysis.

formed near the leading edge (A_S) and the maximum u-fluctuation amplitudes of T-S waves excited downstream (A_{TS}). The amplitude of oscillating Mach wave is the amplitude at the leading edge position without the boundary layer plate. Maslov et al.[8] measured the coupling coefficient defined as the amplitude ratio of T-S wave to the oscillating Mach wave (A_{TS}/A_M). Table 1 shows that A_{TS}/A_M varies from 0.37 to 1.84, while A_{TS}/A_S is almost of unity. Thus, it is concluded that the strength of the excited T-S wave is determined by the Stokes layer induced by the incident Mach wave in the vicinity of the leading edge. The amplitude of the Stokes layer is almost the same as the u-fluctuation amplitude on the wall just behind the leading edge for the inviscid flow, which can be calculated on the basis of the potential flow theory.

4 Conclusion

We have presented our simulation results for supersonic boundary layer receptivity to oscillating Mach waves incident onto leading edge of the plate at freestream Mach number 2.2.

The results show that the oscillating Stokes layer is induced by the incident Mach wave near the leading edge, and it develops into T-S wave. The amplitude ratio of the excited T-S wave to the Stokes layer in the vicinity of the leading

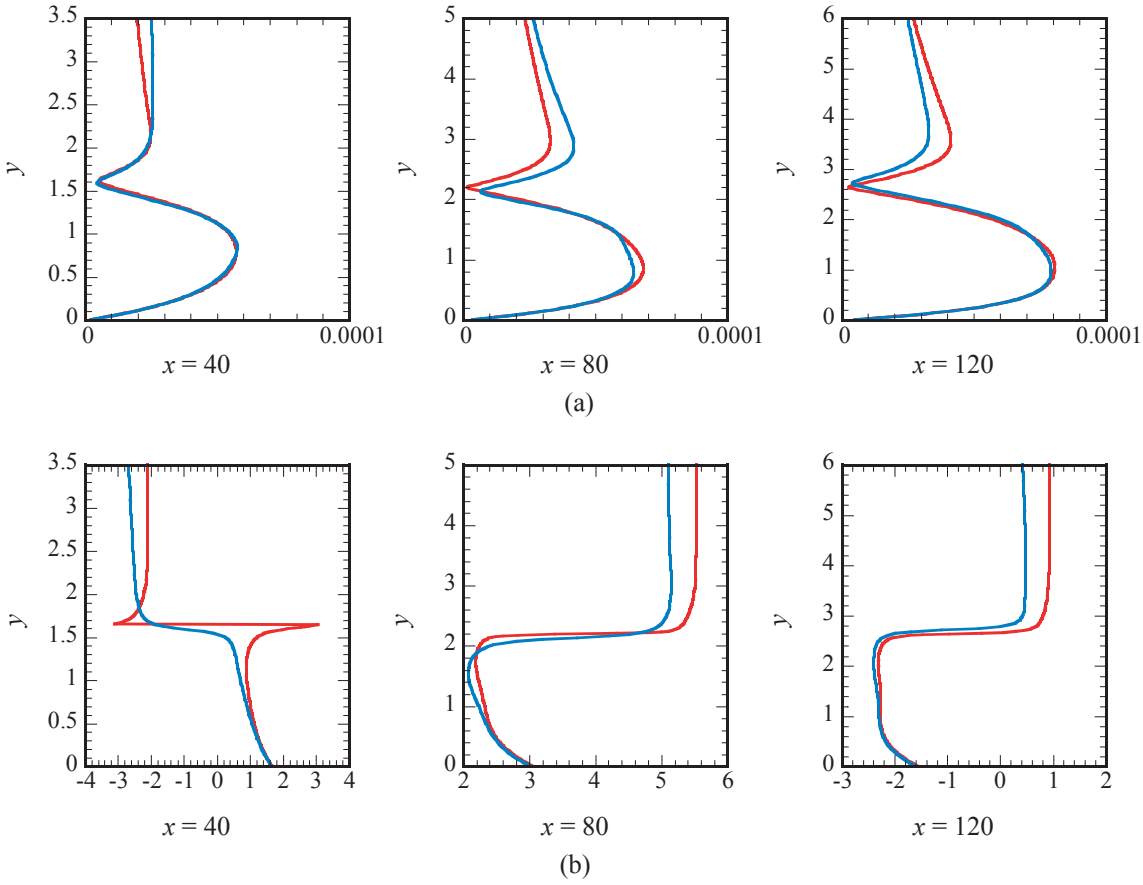

Fig.4 (continued).

edge is almost of unity.

Acknowledgments

This work is partly supported by a Grant-in-Aid for Scientific Research (No. 12125203 and No. 14750722) from the Ministry of Education, Science and Culture, Japan.

References

[1] Nishioka, M., Morkovin, M., Boundary-layer receptivity to unsteady pressure gradients: experiments and overview. *J. Fluid Mech.*, 171, 219-261, 1986.

[2] Sakaue, S., Nishioka, M., On the receptivity process generating Tollmein-Schlichting waves in supersonic laminar boundary layer. *Proc. 7th ACFM*, 271-274, 1997.

[3] Asai, M., Nishioka, M., A numerical study on the receptivity process generating Tollmien-Schlichting waves. *Fluid Dynamics Research*, 12, 229-239, 1993.

[4] Choudhari, M., Streett, C., Boundary layer receptivity phenomena in three-dimensional and high-speed boundary layers. AIAA 90-5258, 1990.

[5] Mack, L. M., Boundary-layer linear stability theory. *Special Course on Stability and Transitionif Laminar Flow. AGARD Rep*. No. 709, 1-81, 1987.

[6] Fedorov, A. V., Receptivity of a high-speed boundary layer to acoustic disturbances. *J. Fluid Mech*., vol.491, 101-129, 2003.

[7] Kendall, J. M., Wind tunnel experiments relating to supersonic and hypersonic boundary layer transition. *AIAA J.*, 13, 3, 290-299, 1975.

[8] Maslov, A. A., Shiplyuk, A. N., Sidorenko, A. A., Arnal, D., Leading-edge receptivity of a hypersonic

boundary layer on a flat plate. *J. Fluid Mech.*, vol. 426, 73-94, 2001.

[9] Zhong, X., Leading-edge receptivity to free-stream disturbance waves for hypersonic flow over a parabola. *J. Fluid Mech.,* vol.441, 315-367, 2001..

[10] Malik, M. R., Lin, R., Sengupta, R., Computation of hypersonic boundary-layer response to external disturbnaces. AIAA 99-0411, 1999.

[11] Sakaue, S., Asai, M., Nishioka, M., On the receptivity process of supersonic laminar boundary layer. *Laminar-Turbulent Transition*, Springer, 481-486, 2000.

[12] Sakaue, S., Nishioka, M., Supersonic boundary layer receptivity to Mach waves incident onto leading-edge. *Proc 9th ACFM,* CD-ROM 53, 2002.

[13] Ma, Y., Zhong, X., Receptivity of a supersonic boundary layer over a flat plate. Part 1. Wave structures and interactions. *J. Fluid Mech.*, 488, 31-78, 2003.

[14] Chakravarthy, S. R., Osher, S., A new class of high accuracy TVD schemes for hyperbolic conservation laws. AIAA 85-0363, 1985.

Table 1 u-fluctuation amplitude ($\times 10^{-4}$)

	Mach wave:A_M (x = 0.0)	Stokes layer:A_S (x = 2.0)	TS wave:A_{TS} (x = 24.0)	A_{TS}/A_M	A_{TS}/A_S
Case1	3.639	1.138	1.359	0.373	1.194
Case2	1.448	0.724	0.878	0.607	1.213
Case3	1.913	2.895	3.516	1.838	1.215
Case4	1.092	0.940	0.934	0.855	0.994